0026-895X/04/6505-1269–1277$20.00
MOLECULAR PHARMACOLOGY
Vol. 65, No. 5
2862/1146853
Mol Pharmacol 65:1269–1277, 2004
Printed in U.S.A.
Copyright © 2004 The American Society for Pharmacology and Experimental Therapeutics

$Ca_v1.3$ Is Preferentially Coupled to Glucose-Induced $[Ca^{2+}]_i$ Oscillations in the Pancreatic β Cell Line INS-1

Guohong Liu, Nathan Hilliard, and Gregory H. Hockerman

Department of Medicinal Chemistry and Molecular Pharmacology, School of Pharmacy and Pharmacal Sciences (G.L., N.H., G.H.), and the Graduate Program in Neuroscience (G.L.), Purdue University, West Lafayette, Indiana

Received July 30, 2003; accepted February 5, 2004

This article is available online at http://molpharm.aspetjournals.org

ABSTRACT

The link between Ca^{2+} influx through the L-type calcium channels $Ca_v1.2$ or $Ca_v1.3$ and glucose- or KCl-induced $[Ca^{2+}]_i$ mobilization in INS-1 cells was assessed using the calcium indicator indo-1. Cells responded to 18 mM glucose or 50 mM KCl stimulation with different patterns in $[Ca^{2+}]_i$ increases, although both were inhibited by 10 μM nifedipine. Although KCl elicited a prolonged elevation in $[Ca^{2+}]_i$, glucose triggered oscillations in $[Ca^{2+}]_i$. $Ca_v1.2$/dihydropyridine-insensitive (DHPi) cells and $Ca_v1.3$/DHPi cells, and stable INS-1 cell lines expressing either DHP-insensitive $Ca_v1.2$ or $Ca_v1.3$ channels showed normal responses to glucose. However, in 10 μM nifedipine, only $Ca_v1.3$/DHPi cells maintained glucose-induced $[Ca^{2+}]_i$ oscillation. In contrast, both cell lines exhibited DHP-resistant $[Ca^{2+}]_i$ increases in response to KCl. The percentage of cells responding to glucose was not significantly decreased by nifedipine in $Ca_v1.3$/DHPi cells but was greatly reduced in $Ca_v1.2$/DHPi cells. In 10 μM nifedipine, KCl-elicited $[Ca^{2+}]_i$ elevation was retained in both $Ca_v1.2$/DHPi and $Ca_v1.3$/DHPi cells. In INS-1 cells expressing the intracellular II-III loop of $Ca_v1.3$, glucose failed to elicit $[Ca^{2+}]_i$ changes, whereas INS-1 cells expressing the $Ca_v1.2$ II-III loop responded to glucose with normal $[Ca^{2+}]_i$ oscillation. INS-1 cells expressing $Ca_v1.2$/DHPi containing the II-III loop of $Ca_v1.3$ demonstrated a nifedipine-resistant slow increase in $[Ca^{2+}]_i$ and nifedipine-resistant insulin secretion in response to glucose that was partially inhibited by diltiazem. Thus, whereas the II-III loop of $Ca_v1.3$ may be involved in coupling Ca^{2+} influx to insulin secretion, distinct structural domains are required to mediate the preferential coupling of $Ca_v1.3$ to glucose-induced $[Ca^{2+}]_i$ oscillation.

Insulin secretion in response to glucose in pancreatic β cells requires intracellular Ca^{2+} concentration ($[Ca^{2+}]_i$) elevation. The generally accepted model is that glucose metabolism results in the activation of voltage-dependent Ca^{2+} channels (VDCCs), and Ca^{2+} influx causes an increase in $[Ca^{2+}]_i$ that subsequently triggers insulin exocytosis via a poorly understood mechanism. Different patterns of $[Ca^{2+}]_i$ increases have been observed in β cells, which can be generally described as $[Ca^{2+}]_i$ oscillations with diverse frequency and amplitude (Theler et al., 1992; Hellman et al., 1994) or sustained $[Ca^{2+}]_i$ increases without oscillation (Grapengiesser et al., 1992; Theler et al., 1992). The contribution of both patterns of $[Ca^{2+}]_i$ increase to insulin secretion is not clear (Westerlund et al., 1997; Bergsten, 1998; Kjems et al., 2002). However, observation of a temporal correlation between $[Ca^{2+}]_i$ oscillation and insulin secretion in pancreatic β cells suggests the functional importance of glucose-induced $[Ca^{2+}]_i$ oscillation (Bergsten et al., 1994; Soria and Martin, 1998; Ravier et al., 1999).

The mechanisms leading to glucose-induced $[Ca^{2+}]_i$ oscillation and the source of the Ca^{2+} mobilized during oscillations are not clear, although Ca^{2+} influx across the plasma membrane seems to be required (Devis et al., 1975a). Among the multiple calcium-conducting channels expressed on the plasma membrane of pancreatic β cells, the critical role of

This work was supported by American Diabetes Association Research Award 1119990378 (to G.H.H.).

ABBREVIATIONS: $[Ca^{2+}]_i$, intracellular Ca^{2+} concentration; $Ca_v1.2$/II-III cells, INS-1 cells stably transfected with the $Ca_v1.2$ intracellular II-III loop fused to green fluorescent protein; $Ca_v1.3$/II-III cells, INS-1 cells stably transfected with the $Ca_v1.3$ intracellular II-III loop fused to green fluorescent protein; $Ca_v1.2$/DHPi, dihydropyridine-insensitive $Ca_v1.2$ fused to green fluorescent protein; $Ca_v1.3$/DHPi, dihydropyridine-insensitive $Ca_v1.3$ fused to green fluorescent protein; $Ca_v1.2$/DHPi/1.3II-III, dihydropyridine-insensitive $Ca_v1.2$ containing the II-III loop of $Ca_v1.3$, fused to green fluorescent protein; $Ca_v1.2$/DHPi cells, INS-1 cells stably transfected with the $Ca_v1.2$/dihydropyridine-insensitive channel; $Ca_v1.3$/DHPi cells, INS-1 cells stably transfected with the $Ca_v1.3$/dihydropyridine-insensitive channel; $Ca_v1.2$/DHPi/1.3II-III cells, INS-1 cells stably transfected with the $Ca_v1.2$/dihydropyridine-insensitive/1.3II-III channel; DHP, dihydropyridine; DHPi, dihydropyridine-insensitive; GFP, green fluorescent protein; indo-1 AM, (4-(6-carboxy-2-indolyl)-4′-methyl-2.2′-(ethylenedioxy)dianiline-*N,N,N′,N′*-tetraacetic acid tetrakis(acetoxymethyl) ester); VDCC, voltage-dependent calcium channels; ER, endoplasmic reticulum; RT-PCR, reverse transcription-polymerase chain reaction; PCRpolymerase chain reaction; ANOVA, analysis of variance; KRBH, Krebs-Ringer-bicarbonate HEPES; MES, methanesulfonic acid.

MOLECULAR PHARMACOLOGY

Downloaded from molpharm.aspetjournals.org at ASPET Journals on February 26, 2020

L-type VDCC in mediating $[Ca^{2+}]_i$ increase and insulin secretion has been long established (Devis et al., 1975b; Dukes and Cleemann, 1993). Previously, we reported that one isoform of L-type VDCC, $Ca_v1.3$, is preferentially coupled to glucose-induced insulin secretion (Liu et al., 2003). However, the underlying mechanism for this coupling, as well as the relative contribution of $Ca_v1.2$ (Seino et al., 1992; Horvath et al., 1998) and $Ca_v1.3$ (Seino et al., 1992) to $[Ca^{2+}]_i$ mobilization in β cells, is still poorly understood.

Ca^{2+} entry via plasma membrane channels may not exclusively account for the glucose-triggered $[Ca^{2+}]_i$ oscillation because some evidence supports the participation of the internal Ca^{2+} pool in this event (Roe et al., 1993; Gilon et al., 1999; Arredouani et al., 2002). Multiple types of Ca^{2+} release channels are expressed on the ER membrane of β cells (Islam et al., 1992; Bruton et al., 2003; Lemmens et al., 2001). In addition to Ca^{2+} influx via VDCC and Ca^{2+} release from ER, multiple ion conductances may contribute to the regulation of β cell membrane potential and glucose-induced $[Ca^{2+}]_i$ oscillation (Fridlyand et al., 2003). Furthermore, ATP-sensitive potassium current (Larsson et al., 1996), calcium-activated potassium current (Gopel et al., 1999), and calcium-release–activated nonselective cation current (Roe et al., 1998) may all play a role in oscillations in membrane potential that could, in turn, be influenced by the release of Ca^{2+} from internal stores or the associated metabolic activity.

The present study was undertaken to investigate the role of two distinct L-type VDCCs, $Ca_v1.2$ and $Ca_v1.3$, in $[Ca^{2+}]_i$ changes in response to glucose or KCl stimulation in the rat pancreatic β cell line INS-1. INS-1 cells express both $Ca_v1.2$ and $Ca_v1.3$ channels (Horvath et al., 1998), which are not readily differentiated by pharmacological agents. Therefore, we used INS-1 cell lines stably transfected with dihydropyridine-insensitive $Ca_v1.2$ (Cav1.2/DHPi cells) or $Ca_v1.3$ ($Ca_v1.3$/DHPi cells) channels (Liu et al., 2003). In these cell lines, endogenous L-type channels can be "turned off" with a DHP such as nifedipine, functionally isolating the drug-insensitive $Ca_v1.2$ or $Ca_v1.3$ mutant. Upon exposure to 18 mM glucose, $Ca_v1.3$/DHPi cells but not $Ca_v1.2$/DHPi cells exhibited nifedipine-resistant $[Ca^{2+}]_i$ oscillation. In contrast, DHP-insensitive $[Ca^{2+}]_i$ elevation induced by KCl was maintained in both $Ca_v1.2$/DHPi and $Ca_v1.3$/DHPi cells. Furthermore, overexpression of the intracellular loop linking domains II and III of $Ca_v1.3$ inhibited glucose-induced $[Ca^{2+}]_i$ oscillation, whereas the overexpression of the corresponding loop from $Ca_v1.2$ did not. Finally, a chimeric $Ca_v1.2$/DHPi channel containing the II-III loop of $Ca_v1.3$ is more efficiently coupled to KCl-stimulated insulin secretion than is the $Ca_v1.2$/DHPi channel and is capable of mediating glucose-stimulated insulin secretion but not glucose-stimulated $[Ca^{2+}]_i$ oscillations. These results indicate that the Ca^{2+} influx through $Ca_v1.3$ is preferentially linked to glucose-induced $[Ca^{2+}]_i$ oscillation, and the intracellular II-III loop of $Ca_v1.3$ may be involved in this specific linkage but is not sufficient to transfer this property to $Ca_v1.2$. These data are in agreement with our previous results studying insulin secretion (Liu et al., 2003), and hence, $Ca_v1.3$-mediated $[Ca^{2+}]_i$ oscillation in response to glucose is proposed as the mechanism for the coupling of $Ca_v1.3$ to glucose-stimulated insulin secretion.

Materials and Methods

Cell Culture and Transfection. INS-1 cells were cultured as described previously (Asfari et al., 1992). The creation and characterization of the stable INS-1 cell lines $Ca_v1.2$/DHPi, $Ca_v1.3$/DHPi, $Ca_v1.2$/II-III, and $Ca_v1.3$/II-III were reported previously (Liu et al., 2003). Cells were cultured for at least 2 weeks after thawing before experiments were performed. Because insulin secretion in INS-1 cells diminishes over time in culture, only cells between passage 30 and 80 were used in experiments.

Construction of $Ca_v1.2$/DHPi/1.3II-III Channel cDNA. The II-III loop of $Ca_v1.2$/DHPi was replaced with a short sequence containing the restriction sites HpaI and SwaI using the oligonucleotide pair (5′ to 3′) CTGGCTGATGCGGAGTCGTTAACTAATTTAAATCTCATC-CTCTTCTTCATTCTG and GAAGAAGAGGATGAGATTTAAATT-AGTTAACGACTCCGCATCAGCCAGGTTGTC. The II-III loop of $Ca_v1.3$ was amplified with flanking DraI (5′) and PmlI (3′) sites using the oligonucleotide pair (5′ to 3′) TTTATTTAAACACTGCTCAGAAA-GAAGAAGCGGAAGAAAAGG and TTTACACGTGAAGATGTGGTG-GTTGATGAGCTTGTGGCAGCC. The restriction sites were cut, and the $Ca_v1.3$ loop was ligated into $Ca_v1.2$/DHPi. Products were screened for the presence and orientation of the $Ca_v1.3$ II-III loop and sequenced. The chimera represents amino acids 763 to 905 of $Ca_v1.2$/DHPi replaced by amino acids 762 to 888 of $Ca_v1.3$.

Stable Transfection. INS-1 cells were transfected with cDNA encoding the $Ca_v1.2$/DHPi/1.3II-III channel ligated into the plasmid vector pcDNA3 (Invitrogen, Carlsbad, CA) using GenePorterII (GeneTherapy Systems, San Diego, CA). After 3 days, 100 μg/ml G418 (Promega, Madison, WI) was added to the medium. Colonies were isolated and subsequently screened by RT-PCR and Western blot.

RT-PCR. Total RNA was extracted from INS-1 cells using TRIzol (Invitrogen), and 2 μg was incubated with random primers at 70°C for 5 min and then put on ice. RNase inhibitor (1 μl), 500 μM dNTPs, 0.01 M dithiothreitol, and 200 U Moloney murine leukemia virus reverse transcriptase (Promega) were added to the mixture (final volume, 25 μl) and incubated at 37°C for 60 min. Two primer pairs were used for PCR with Taq polymerase (Promega): primer set $Ca_v1.2$CT (5′-agc tgt gta tat gcc ctg g-3′) and GFPr (5′-gaa gaa gtc gtg ctg ctt c-3′). The $Ca_v1.2$CT and GFPr primers were used to amplify the channel/enhanced GFP junction. The predicted PCR product is 344 base pairs for $Ca_v1.2$/DHPi/1.3II-III. PCR products were visualized by ethidium bromide staining after 1% agarose gel electrophoresis in 40 mM Tris-acetate and 2 mM EDTA, pH 8.5.

Western Blot. Crude Membranes from indicated cells were isolated as described previously (Peterson et al., 1997). For whole-cell lysates, indicated cells were incubated in SDS lysis buffer (0.5% SDS, 0.05M Tris-Cl, and 1 mM dithiothreitol, pH 8.0) for 10 min. Lysates were boiled for 5 min and clarified by centrifugation at 26,000*g* at 4°C for 90 min, and supernatants were collected for Western blot. The proteins were separated by SDS-polyacrylamide gel electrophoresis (5% gels for crude membranes and 12% gels for cell lysates) followed by transfer to nitrocellulose membrane. The membranes were blocked with 5% nonfat milk in Tris-buffered saline at 4°C overnight, washed with 0.1% Tween-20 in Tris-buffered saline, and incubated with the polyclonal rabbit antibodies against the C-terminal tail of $Ca_v1.2$ (CNC2; Hell et al., 1993b) for 2–3 h. The blots were detected by incubation with horseradish peroxidase-conjugated anti-rabbit antibodies and visualized by enhanced chemiluminescence with Hyperfilm (Amersham Biosciences AB, Uppsula, Sweden). Protein concentrations were determined using the Bradford assay (Bio-Rad, Hercules, CA).

Electrophysiology. Whole-cell barium currents were recorded at room temperature using an Axopatch 200B amplifier (Axon Instruments Inc., Union City, CA) and filtered at 1 kHz (six-pole Bessel filter, −3 dB). Electrodes were pulled from borosilicate glass (VWR, West Chester, PA) and fire-polished to resistances of 2 to 6 MΩ. Voltage pulses were applied, and data were acquired using pClamp8

Downloaded from molpharm.aspetjournals.org at ASPET Journals on February 26, 2020

software (Axon Instruments). Nifedipine and diltiazem (Sigma/RBI, Natick, MA) were applied to the recording chamber in bath saline at 0.5 ml/min. The bath saline contained 150 mM Tris, 10 mM $BaCl_2$, and 4 mM $MgCl_2$. The intracellular solution contained 130 mM *N*-methyl-D-glucamine, 10 mM EGTA, 60 mM HEPES, 2 mM MgATP, 1 mM $MgCl_2$. The pH of both solutions was adjusted to 7.3 with MES.

Insulin Secretion Assay. Glucose- (11.2 mM) and KCl- (50 mM) stimulated insulin secretion was assayed in $Ca_v1.2$/DHPi/1.3II-III cells as reported previously (Liu et al., 2003) and expressed as a percentage of cell content.

Measurement of $[Ca^{2+}]_i$. INS-1 cells were split into four-well, glass-bottomed chambers (Nalge Nunc International, Naperville, IL) and cultured in complete medium for 48 h before experiments. Cells were washed with Krebs-Ringer-bicarbonate HEPES (KRBH) buffer (115 mM NaCl, 24 mM $NaHCO_3$, 5 mM KCl, 1 mM $MgCl_2$, 2.5 mM $CaCl_2$, 25 mM HEPES, and 0.5% bovine serum albumin, pH 7.4), and incubated with 5 μM of the calcium indicator indo-1 AM (Molecular Probes, Eugene, OR) in KRBH buffer for 30 min in the dark. After washing with KRBH buffer, cells were incubated for an additional 30 min in KRBH buffer. Indo-1 AM-loaded cells in glass-bottomed chambers were observed via confocal laser scanning microscopy with an MRC 1024 (Bio-Rad) system based on an inverted Diaphot 300 microscope (Nikon, Tokyo, Japan). The stage was thermostatically controlled to maintain a temperature of 37°C in the bottom of the chamber. The confocal system was equipped with a 60× PlanApo 1.4 numerical aperture oil immersion objective lens and 100-mW argon ion water-cooled laser (Coherent Inc., Santa Clara, CA). Single cells or small clusters of cells, isolated optically by means of a diaphragm, were studied by indo-1 fluorescence. Indo-1 AM-loaded cells were excited at 363 nM, and the emission at wavelengths of 405 (F_{405}) and 460 nm (F_{460}) were used to calculate the fluorescence ratio (F_{405}/F_{460}). Cells were excited at a frequency of 1 Hz, and the fluorescence images were collected simultaneously. $[Ca^{2+}]_i$ was calculated from F_{405}/F_{465} using a standard curve generated with a Ca^{2+} concentration buffer kit with Mg^{2+} (Molecular Probes).

Data Analysis. The time courses of the fluorescence values (F_{405} and F_{460}) from each cell were obtained using Lasersharp software (Bio-Rad). The ratios (F_{405}/F_{460}) and $\int\Delta\ [Ca^{2+}]_i \cdot dt$ were calculated, and final figures were presented using Sigmaplot 8.01 (SPSS Inc., Chicago, IL). Electrophysiological data were analyzed using Clampfit 8.1 (Axon Instruments) and Sigma Plot 8.01. Results are presented as means ± S.E. for the number of observations as indicated. The statistical significance of differences between two groups was determined using Student's unpaired *t* test, with $p < 0.05$ considered significant. The statistical significance of differences among multiple experimental groups was determined using one-way ANOVA and the Tukey post hoc test, with $p < 0.05$ considered significant.

Results

Previously, we identified $Ca_v1.3$ as the prominent L-type VDCC in mediating glucose-induced insulin secretion in INS-1 cells (Liu et al., 2003). However, the underlying mechanism for the preferential coupling between $Ca_v1.3$ and glucose-induced insulin secretion remained unclear. Because glucose-stimulated increases in $[Ca^{2+}]_i$ are tightly correlated with insulin secretion, we measured changes in $[Ca^{2+}]_i$ in untransfected INS-1 cells and the stable, INS-1-derived cell lines $Ca_v1.2$/DHPi and $Ca_v1.3$/DHPi in response to either 18 mM glucose or 50 mM KCl. In INS-1 cells, both 18 mM glucose and 50 mM KCl-induced $[Ca^{2+}]_i$ changes over time were recorded using the Ca^{2+} indicator indo-1 AM (Fig. 1). As shown in Fig. 1A, glucose stimulation initiated oscillations in $[Ca^{2+}]_i$ of varied frequency and amplitude. In contrast, KCl stimulation induced only a single transient $[Ca^{2+}]_i$ increase that returned to basal levels over the course of 2 to 3 min (Fig. 1B). Both the glucose- and KCl-stimulated increases in $[Ca^{2+}]_i$ were inhibited by the application of 10 μM nifedipine, an L-type VDCC blocker (Fig. 1, A and B).

To investigate whether calcium influx via the two distinct L-type VDCCs $Ca_v1.2$ and $Ca_v1.3$ is differentially coupled to changes in $[Ca^{2+}]_i$, glucose- and KCl-stimulated $[Ca^{2+}]_i$ increases were studied in $Ca_v1.2$/DHPi cells and $Ca_v1.3$/DHPi cells (Fig. 2), which are INS-1 cells stably expressing DHP-insensitive $Ca_v1.2$ or $Ca_v1.3$ (Liu et al., 2003). In $Ca_v1.2$/DHPi cells, both glucose and KCl elicited the expected patterns of $[Ca^{2+}]_i$ changes in the absence of nifedipine (Fig. 2, A and C). In the presence of 10 μM nifedipine, the KCl-stimulated increase in $[Ca^{2+}]_i$ was retained, although at a reduced amplitude (Fig. 2C). However, in the presence of 10 μM nifedipine, glucose stimulation of $Ca_v1.2$/DHPi cells only elicited a transient increase in $[Ca^{2+}]_i$, with no subsequent $[Ca^{2+}]_i$ oscillations (Fig. 2A). These data clearly show that the normal glucose and KCl-stimulated changes in $[Ca^{2+}]_i$ are intact in $Ca_v1.2$/DHPi cells, but under conditions in which only $Ca_v1.2$ channels are activated (in the presence of nifedipine), only the KCl-initiated increase in $[Ca^{2+}]_i$ is observed.

The changes of $[Ca^{2+}]_i$ were also examined in $Ca_v1.3$/DHPi cells (Fig. 2, B and D). As expected, glucose initiated $[Ca^{2+}]_i$ oscillations in the absence of nifedipine. However, in contrast to $Ca_v1.2$/DHPi cells, $Ca_v1.3$/DHPi cells showed nifedipine-resistant calcium oscillation in response to glucose (Fig. 2B). As in $Ca_v1.2$/DHPi cells, the KCl-stimulated monophasic increase in $[Ca^{2+}]_i$ was also retained in $Ca_v1.3$/DHPi cells in the presence of nifedipine (Fig. 2, B and D). Thus, whereas

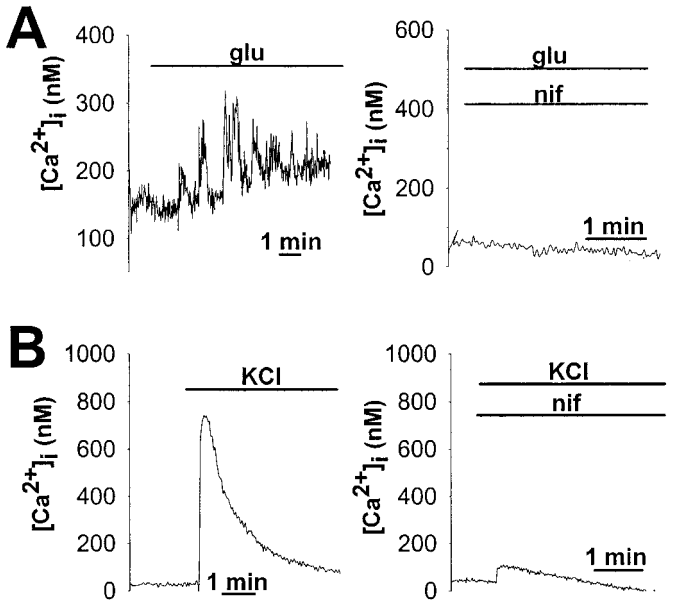

Fig. 1. $[Ca^{2+}]_i$ response to glucose (glu) or KCl in untransfected INS-1 cells Glucose triggered $[Ca^{2+}]_i$ oscillation in INS-1 cells, whereas KCl induced a monophasic $[Ca^{2+}]_i$ increase. Both were sensitive to the L-type VDCC blocker nifedipine (nif). A, glucose-induced $[Ca^{2+}]_i$ oscillation in INS-1 cells. Left, 18 mM glucose elicited multiple phases of $[Ca^{2+}]_i$ increase. The frequency and amplitude of this $[Ca^{2+}]_i$ oscillation showed variation from cell to cell. Right, glucose-induced $[Ca^{2+}]_i$ oscillation was completely blocked by 10 μM nifedipine. B, KCl-induced $[Ca^{2+}]_i$ elevation in INS-1 cells. Left, 50 mM KCl induced a single transient phase of $[Ca^{2+}]_i$ increase in INS-1 cells. Right, 10 μM nifedipine inhibited the response to KCl. Data shown in both A and B are representative traces from single-cell measurements.

Downloaded from molpharm.aspetjournals.org at ASPET Journals on February 26, 2020

both $Ca_v1.2$/DHPi and $Ca_v1.3$/DHPi cells support DHP-resistant $[Ca^{2+}]_i$ increases in response to KCl, activation of $Ca_v1.3$, but not $Ca_v1.2$, is specifically linked to glucose-induced $[Ca^{2+}]_i$ oscillation in INS-1 cells.

The observed $[Ca^{2+}]_i$ oscillation in response to glucose in INS-1 cells is of varied frequency and amplitude, with frequencies in the 1 to 8 oscillations/min range and peak amplitudes in the 200 to 800 nM range. Because of the heterogeneous nature of the cell's response to glucose, we compared the percentage of cells actively oscillating upon glucose stimulation in untransfected INS-1, $Ca_v1.2$/DHPi, and $Ca_v1.3$/DHPi cells (Fig. 3A). In untransfected INS-1 cells, ~60% of cells responded to 18 mM glucose stimulation with $[Ca^{2+}]_i$ oscillations, which decreased to ~3% of cells responding in the presence of nifedipine. In $Ca_v1.2$/DHPi cells, the percentage of cells demonstrating glucose-induced $[Ca^{2+}]_i$ oscillation was ~50% and 0% in the absence and presence of 10 μM nifedipine, respectively. However, nifedipine failed to significantly inhibit glucose-stimulated $[Ca^{2+}]_i$ oscillation in $Ca_v1.3$/DHPi cells (~60% without nifedipine and ~50% with nifedipine).

Upon 50 mM KCl stimulation, virtually 100% of INS-1 cells exhibited $[Ca^{2+}]_i$ elevation. For quantitative comparison of $[Ca^{2+}]_i$ responses in untransfected INS-1, $Ca_v1.2$/DHPi, and $Ca_v1.3$/DHPi cells, we calculated the integral of the augmentation in $[Ca^{2+}]_i$ over time ($\int\Delta\ [Ca^{2+}]_i \cdot dt$) after depolarization (Fig. 3B). A period of 200 s was chosen for calculating the Ca^{2+} integral because during sustained exposure to KCl, $[Ca^{2+}]_i$ usually returned to near basal levels by this time. In untransfected INS-1 cells in the presence of nifedipine, the $\int\Delta\ [Ca^{2+}]_i \cdot dt$ measured during 200 s of depolarization was substantially lower than that of INS-1 cells in the absence of nifedipine (22,592 $\pm$ 3209 and 2563 $\pm$ 290 in the presence or absence of nifedipine, respectively). Nifedipine also suppressed the $[Ca^{2+}]_i$ increase in $Ca_v1.2$/DHPi cells and $Ca_v1.3$/DHPi cells, but the remaining DHP-insensitive $[Ca^{2+}]_i$ increase is significantly higher than basal level. These results quantitatively demonstrate that both $Ca_v1.2$ and $Ca_v1.3$ are able to mediate KCl-induced $[Ca^{2+}]_i$ elevation, but only $Ca_v1.3$ is involved in glucose-triggered $[Ca^{2+}]_i$ oscillations.

The intracellular loops linking domains II and III of $Ca_v1.2$ and $Ca_v1.3$ are much less conserved than other regions of these channels and are probably determinants of specificity of function. We have previously shown, using INS-1 cells stably transfected with either the II-III loop of $Ca_v1.2$ ($Ca_v1.2$/II-III cells) or $Ca_v1.3$ ($Ca_v1.3$/II-III cells), that overexpression of the $Ca_v1.3$ II-III loop inhibits glucose-stimulated insulin secretion (Liu et al., 2003). To further investigate whether this portion of the channel is also important for coupling of $Ca_v1.3$ to glucose-stimulated $[Ca^{2+}]_i$ oscillation, changes in $[Ca^{2+}]_i$ in response to glucose and KCl were studied in $Ca_v1.2$/II-III cells and $Ca_v1.3$/II-III cells (Fig. 4). Similar to untransfected INS-1 cells, $Ca_v1.2$/II-III cells responded to glucose with normal $[Ca^{2+}]_i$ oscillation (Fig. 4A). However, no $[Ca^{2+}]_i$ oscillation was observed in $Ca_v1.3$/II-III cells upon glucose stimulation (Fig. 4B). In contrast, both cell lines responded to 50 mM KCl with similar increases in $[Ca^{2+}]_i$ (Fig. 4, A and B). Therefore, in agreement with our previous study of insulin secretion in these cell lines, the II-III loop of $Ca_v1.3$ apparently plays a role in glucose-stimulated $[Ca^{2+}]_i$ oscillation.

To determine whether the II-III loop of $Ca_v1.3$ is sufficient to couple $Ca_v1.2$ to glucose-stimulated insulin secretion and $[Ca^{2+}]_i$ oscillations, we constructed a chimeric $Ca_v1.2$/DHPi channel containing the intracellular II-III loop of $Ca_v1.3$ in fusion with green fluorescent protein (GFP) (Fig. 5A). The II-III loops of $Ca_v1.2$ and 1.3 are 135 and 151 amino acids in length, respectively, and are only ~50% identical. INS-1 cells were stably transfected with the chimeric channel cDNA, and clonal cell lines were screened for the presence of chimeric channel mRNA by RT-PCR using primers that bracket the channel C-terminal tail/GFP junction. The presence of the $Ca_v1.2$/DHPi/1.3II-III chimeric protein in one clone was detected by Western blot with an antibody directed against the C-terminal tail of $Ca_v1.2$ (Hell et al., 1993b) as a band with slightly lower mobility upon SDS-polyacrylamide gel electrophoresis than the endogenous $Ca_v1.2$ channel (Fig. 5A). The functional expression of the chimeric channel was confirmed by whole-cell patch-clamp electrophysiology using 10 μM nifedipine to block endogenous L-type channels and 50 μM diltiazem to block the DHP-resistant chimeric channel (Fig. 5B). As we observed in our characterization of the $Ca_v1.2$/DHPi and $Ca_v1.3$/DHPi cell lines, application of 10 μM nifedipine plus 50 μM diltiazem blocked significantly more barium current in $Ca_v1.2$/DHPi/1.3II-III cells than did 10 μM nifedipine alone (Fig. 5C). In contrast, application of 10 μM nifedipine plus 50 μM diltiazem did not block significantly more barium current in untransfected INS-1 cells than did 10

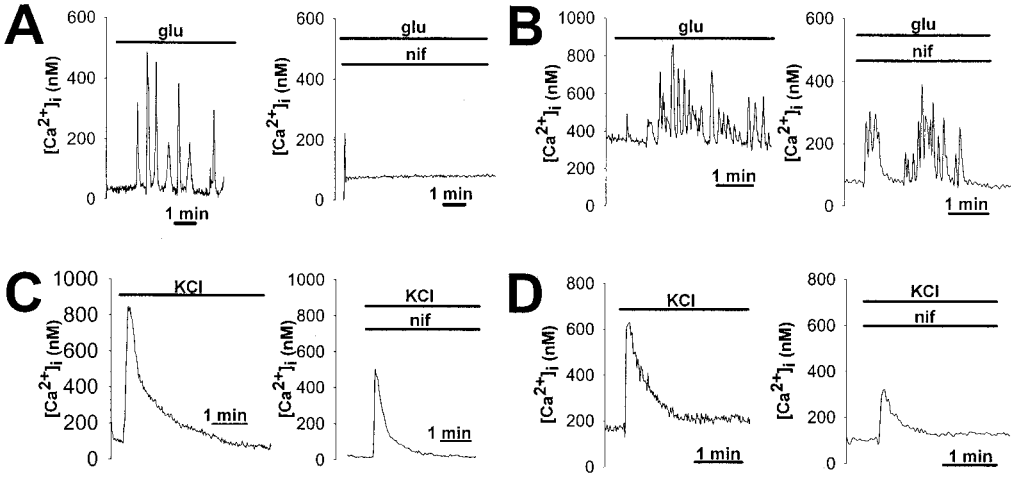

Fig. 2. $[Ca^{2+}]_i$ response to glucose or KCl in $Ca_v1.2$/DHPi and $Ca_v1.3$/DHPi cells. A, as in untransfected INS-1 cells, 18 mM glucose (glu) elicited $[Ca^{2+}]_i$ oscillation in $Ca_v1.2$/DHPi cells. In the presence of 10 μM nifedipine (nif), the $[Ca^{2+}]_i$ oscillation was completely abolished. B, in $Ca_v1.3$/DHPi cells, glucose-induced $[Ca^{2+}]_i$ oscillation was maintained in the presence and absence of 10 μM nifedipine. For both $Ca_v1.2$/DHPi cells (C) and $Ca_v1.3$/DHPi cells (D), a single spike of $[Ca^{2+}]_i$ elevation upon KCl stimulation was observed. In both cell lines, 10 μM nifedipine only partially blocked KCl-induced $[Ca^{2+}]_i$ increase. Data shown are representative traces measured in single cells.

Downloaded from molpharm.aspetjournals.org at ASPET Journals on February 26, 2020

μM nifedipine alone (Liu et al., 2003). In addition, the barium current density in $Ca_v1.2$/DHPi/1.3II-III cells was not significantly greater than that of untransfected INS-1 cells (Fig. 5D). Thus, the chimeric channel is functionally expressed in the $Ca_v1.2$/DHPi/1.3II-III stable cell line, and these cells do not exhibit a significantly greater level of voltage-gated Ca^{2+} channel activity than untransfected INS-1 cells.

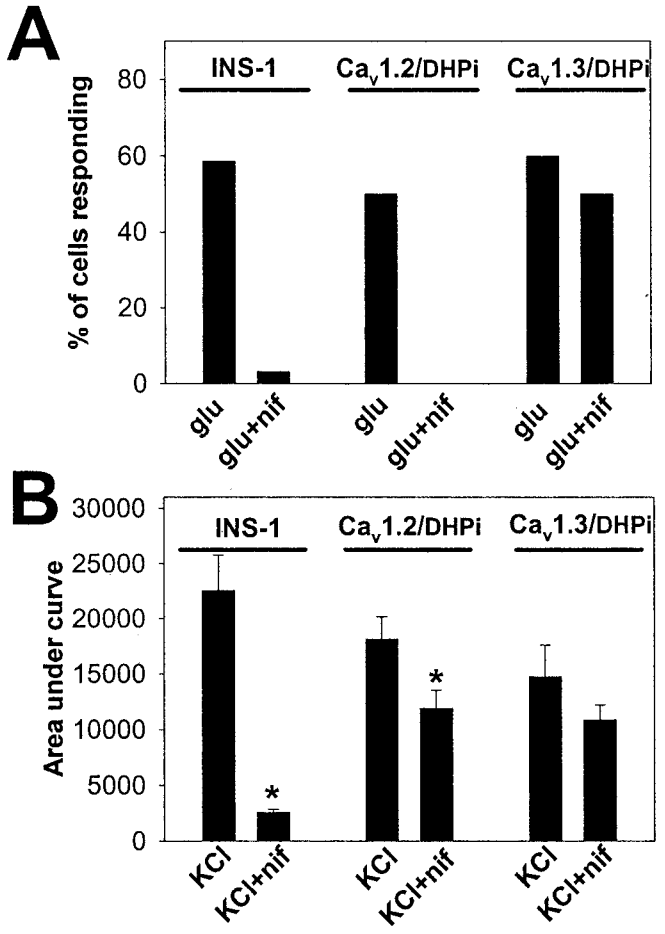

Fig. 3. Quantitative comparison of the $[Ca^{2+}]_i$ response to glucose (glu) or KCl in untransfected INS-1, $Ca_v1.2$/DHPi, and Cav1.3/DHPi cells. A, percentage of cells showing $[Ca^{2+}]_i$ oscillation upon glucose stimulation in untransfected INS-1 cells, $Ca_v1.2$/DHPi cells, and $Ca_v1.3$/DHPi cells. Cells were considered to oscillate if excursions greater than 50 nM above basal $[Ca^{2+}]_i$ were detected during the 200 s after addition of glucose. In untransfected INS-1 cells, 58.6% (17 of 29, from four experimental groups) of cells demonstrated $[Ca^{2+}]_i$ oscillation in response to 18 mM glucose. In the presence of 10 μM nifedipine (nif), only 3.2% (1 of 31, from four experimental groups) cells oscillated upon glucose stimulation. The percentage of $Ca_v1.2$/DHPi cells demonstrating glucose-induced $[Ca^{2+}]_i$ oscillation was 50% (8 of 16, from two experimental groups), which decreased to 0% (0 of 16, from two experimental groups) in the presence of 10 μM nifedipine. Glucose-induced $[Ca^{2+}]_i$ oscillation in 60% (9 of 15, from two experimental groups) of $Ca_v1.3$/DHPi cells, and application of 10 μM nifedipine did not significantly reduce the percentage of responding cells (50%; 6 of 12, from two experimental groups). B, changes of $[Ca^{2+}]_i$ in response to KCl in untransfected INS-1, $Ca_v1.2$/DHPi, and $Ca_v1.3$/DHPi cells. The areas under the KCl-induced $[Ca^{2+}]_i$ elevation curve were calculated as $\int\Delta\ [Ca^{2+}]_i \cdot dt$ during the 200-s period after 50 mM KCl application. The $\int\Delta\ [Ca^{2+}]_i \cdot dt$ was 22,592 $\pm$ 3209 ($n = 8$) in response to KCl. However, the increase in $[Ca^{2+}]_i$ was significantly suppressed to 2563 $\pm$ 290 ($n = 8$) by 10 μM nifedipine. In $Ca_v1.2$/DHPi cells, KCl-induced $[Ca^{2+}]_i$ increases were no longer sensitive to nifedipine [without nifedipine, 18151 $\pm$ 2034 ($n = 8$); with nifedipine, 11,922 $\pm$ 1632 ($n = 7$)]. As in $Ca_v1.2$/DHPi cells, nifedipine was not able to completely block KCl-induced $[Ca^{2+}]_i$ increases in $Ca_v1.3$/DHPi cells [without nifedipine, 14,773 $\pm$ 2848 ($n = 6$); with nifedipine, 10,886 $\pm$ 1353 ($n = 8$)]; $\star$, $p < 0.05$ compared with KCl.

The functional coupling of the $Ca_v1.2$/DHPi/1.3II-III channel to KCl-mediated insulin secretion and $[Ca^{2+}]_i$ increase was examined (Fig. 6). As shown in Fig. 6A, robust KCl-stimulated insulin secretion was detected in $Ca_v1.2$/DHPi/1.3II-III cells, and the majority of this secretion (~73%) was resistant to 10 μM nifedipine. The fraction of KCl-stimulated secretion resistant to nifedipine in $Ca_v1.2$/DHPi/1.3II-III cells was significantly greater than that of $Ca_v1.2$/DHPi cells (~29%) (Liu et al., 2003). The addition of 500 μM diltiazem to the assay completely inhibited secretion. Likewise, the KCl-stimulated $[Ca^{2+}]_i$ transient in $Ca_v1.2$/DHPi/1.3II-III cells was substantially resistant to 10 μM nifedipine but was completely blocked by 500 μM diltiazem (Fig. 6B). The integral of the augmentation in $[Ca^{2+}]_i$ over time ($\int\Delta\ [Ca^{2+}]_i \cdot dt$) after depolarization (Fig. 6C) was significantly greater in the presence of KCl alone or KCl plus nifedipine than in the presence of KCl plus nifedipine plus diltiazem. Thus, $Ca_v1.2$/DHPi/1.3II-III channels are functionally coupled to KCl-stimulated insulin secretion and $[Ca^{2+}]_i$ increases. Furthermore, our data suggest that insertion of the $Ca_v1.3$ II-III loop into $Ca_v1.2$/DHPi increased the fraction of KCl-stimulated insulin secretion mediated by the drug-resistant channel.

We next tested the ability of the $Ca_v1.2$/DHPi/1.3II-III channel to mediate glucose-stimulated events in INS-1 cells (Fig. 7). Figure 7A shows that 11.2 mM glucose stimulated a small but significant increase in insulin secretion over basal (2 mM) glucose in $Ca_v1.2$/DHPi/1.3II-III cells. Similarly, in the presence of 10 μM nifedipine, 11.2 mM glucose stimulated a significant increase in insulin secretion. This increase

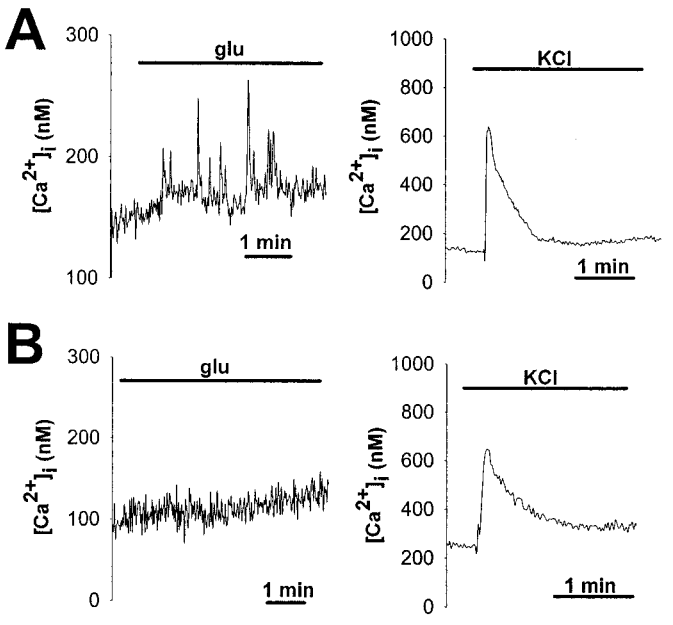

Fig. 4. $[Ca^{2+}]_i$ response to glucose or KCl in $Ca_v1.2$/II-III and $Ca_v1.3$/II-II cells. Overexpression of the intracellular loop linking domains II and III of $Ca_v1.3$ inhibited glucose-induced $[Ca^{2+}]_i$ oscillation but had no effect on KCl-stimulated $[Ca^{2+}]_i$ increase. A, glucose- and KCl-induced $[Ca^{2+}]_i$ increases in $Ca_v1.2$/II-III cells. $Ca_v1.2$/II-III cells responded to 18 mM glucose with $[Ca^{2+}]_i$ oscillation, whereas 50 mM KCl induced a monophasic $[Ca^{2+}]_i$ increase. B, glucose- and KCl-induced changes in $[Ca^{2+}]_i$ in $Ca_v1.3$/II-III cells. Glucose was never observed to elevate $[Ca^{2+}]_i$ in $Ca_v1.3$/II-III cells ($n = 14$ cells in two experimental groups), whereas the KCl-elicited $[Ca^{2+}]_i$ elevation was retained. Data shown in both A and B are representative traces recorded in single cells.

Downloaded from molpharm.aspetjournals.org at ASPET Journals on February 26, 2020

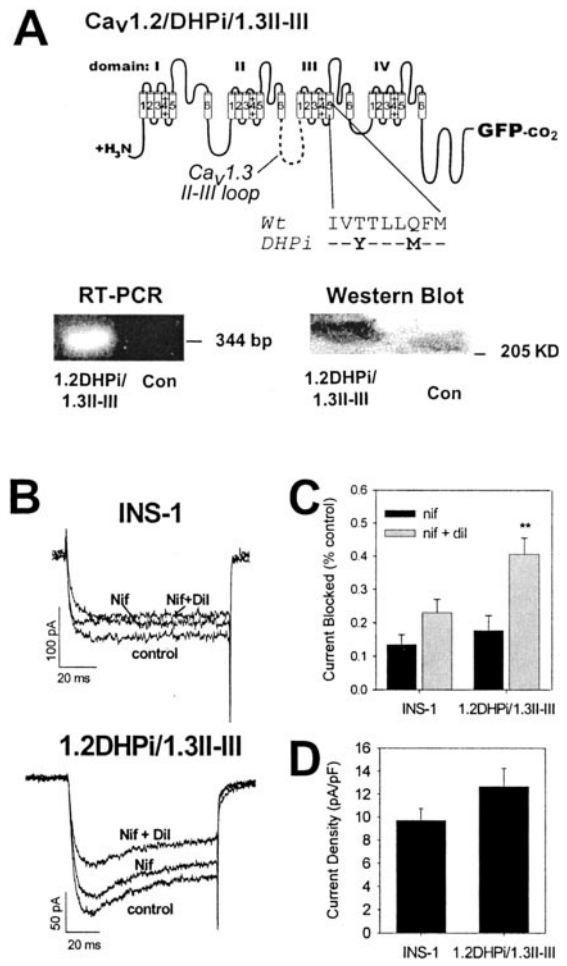

Fig. 5. Characterization of INS-1 cells stably transfected with the chimeric channel $Ca_v1.2$/DHPi/1.3II-III. A, top, Schematic of the chimeric channel $Ca_v1.2$/DHPi/1.3II-III. The dashed lines represent the portion of $Ca_v1.3$ inserted into $Ca_v1.2$. The substitution corresponds to the removal of amino acids 763 to 905 of $Ca_v1.2$, which were replaced by amino acids 762 to 888 of $Ca_v1.3$. The chimera also includes the double point mutation (Thr1039 to Tyr and Gln1043 to Met) in transmembrane segment IIIS5 that renders the channel insensitive to DHPs. GFP is fused to the C-terminal end of the channel. Bottom left, INS-1 cells stably transfected with $Ca_v1.2$/DHPi/1.3II-III cDNA were screened by RT-PCR using primers that flank the channel/GFP junction. The expected 344-base pair fragment is amplified from RNA extracted from transfected cells (1.2DHPi/1.3II-III) but not from untransfected INS-1 cells (control). Bottom right, the presence of the chimeric channel protein was confirmed by Western blot using an antibody raised against a peptide corresponding to the C terminus of $Ca_v1.2$ (Hell et al., 1993b). In crude membrane fractions from INS-1 cells expressing the chimeric channel (1.2/DHPi/1.3II-III), a ~230-kDa protein was detected, whereas a lower apparent molecular weight protein was detected by the same antibody in crude membrane from untransfected INS-1 cells (control). B, representative whole-cell barium currents measured in untransfected INS-1 cells (INS-1), or INS-1 cells stably transfected with the chimeric channel (1.2/DHPi/1.3II-II). The holding potential was −60 mV, with 100-ms depolarizing pulses to +10 mV given every 20 s in the absence (control) or presence of 10 μM nifedipine (nif) or 10 μM nifedipine + 50 μM diltiazem (nif + dil). C, relative fractional blockade of I_{Ba} by drugs. In untransfected INS-1 cells, 13.5 ± 3% (n = 4) of total barium current was blocked by 10 μM nifedipine. Coapplication of 50 μM diltiazem did not significantly reduce DHP-resistant current (23 ± 4%). In $Ca_v1.2$/DHPi/1.3II-III, 10 μM nifedipine blocked 17.7 ± 4.5% (n = 7) of whole-cell current, whereas coapplication of 50 μM diltiazem blocked significantly more current than 10 μM nifedipine alone (41 ± 4%) (n = 7, ⋆⋆, $p < 0.01$). D, barium current density in INS-1 and $Ca_v1.2$/DHPi/1.3II-III cells. Total whole-cell current density (pA/pF) (mean ± S.E.) is shown. There is no statistically significant difference in whole-cell current density between untransfected INS-1 (9.7 ± 1, n = 4) and $Ca_v1.2$/DHPi/1.3II-III cells (12.7 ± 1.6, n = 6).

in insulin secretion was partially inhibited by 500 μM diltiazem. This small amount of nifedipine-resistant, but diltiazem-sensitive, glucose-stimulated insulin secretion observed in $Ca_v1.2$/DHPi/1.3II-III cells contrasts with our previous study in which we observed no nifedipine-resistant, glucose-stimulated insulin secretion in $Ca_v1.2$/DHPi cells (Liu et al., 2003). It is not clear why secretion in response to glucose alone is not significantly different from secretion in response to glucose plus nifedipine plus diltiazem (p = 0.957). However, a nifedipine-resistant, diltiazem-sensitive fraction of glucose-stimulated insulin secretion is clearly de-

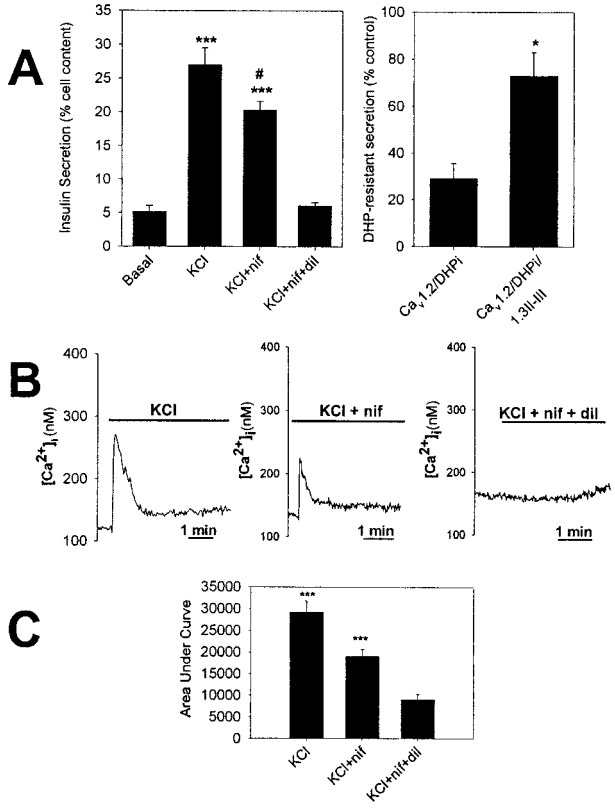

Fig. 6. Insulin secretion and $[Ca^{2+}]_i$ changes in response to 50 mM KCl in $Ca_v1.2$/DHPi/1.3II-III cells. A, insulin secretion (expressed as the percentage of cell content) in response to 50 mM KCl stimulation for $Ca_v1.2$/DHPi/1.3II-III cells: basal = 5.15 ± 0.91%, KCl = 27.03 ± 2.52%, KCl + 10 μM nifedipine (KCl + nif) = 20.35 ± 1.34%, and KCl + 10 μM nifedipine (nif) + 500 μM diltiazem (KCl + nif + dil) = 6.07 ± 0.48% (n = 3–6). Secretion stimulated by 50 mM KCl in both the absence and presence of nifedipine was significantly different from basal secretion (⋆⋆⋆, $p < 0.001$, one-way ANOVA with Tukey post hoc test). Secretion stimulated by 50 mM KCl in the presence of 10 μM nifedipine was significantly different from secretion stimulated by KCl alone (#, $p < 0.05$, one-way ANOVA with Tukey post hoc test). B, $[Ca^{2+}]_i$ increases in response to 50 mM KCl in $Ca_v1.2$/DHPi/1.3II-III cells. KCl stimulation induced a rapid monophasic increase in $[Ca^{2+}]_i$ (left) in virtually every cell. Similar to our observations in $Ca_v1.2$/DHPi and $Ca_v1.3$/DHPi cells, 10 μM nifedipine reduces but does not completely inhibit this response in $Ca_v1.2$/DHPi/1.3II-III cells (middle). Application of 500 μM diltiazem to $Ca_v1.2$/DHPi/1.3II-III cells along with 10 μM nifedipine completely inhibits the 50 mM KCl-stimulated increase in $[Ca^{2+}]_i$ (right). The data shown in B are representative traces from single-cell measurements. C, changes of $[Ca^{2+}]_i$ in response to KCl in $Ca_v1.2$/DHPi/1.3II-III cells. The areas under KCl-induced $[Ca^{2+}]_i$ elevation curves were calculated as $\int\Delta [Ca^{2+}]_i \cdot dt$ during the 200 s immediately following KCl stimulation. The $\int\Delta [Ca^{2+}]_i \cdot dt$ was 29,250 ± 2521 (n = 6) with KCl alone, 19,067 ± 1630 (n = 7) with KCl + 10 μM nifedipine (nif), and 9063 ± 1259 with KCl + 10 μM nifedipine + 500 μM diltiazem (dil) (n = 12). The $\int\Delta [Ca^{2+}]_i \cdot dt$ for KCl and KCl + nif were significantly different from KCl + nif + dil (⋆⋆⋆, $p < 0.001$ one-way ANOVA with Tukey post hoc test).

Downloaded from molpharm.aspetjournals.org at ASPET Journals on February 26, 2020

tected in $Ca_v1.2$/DHPi/1.3II-III cells. Thus, insertion of the $Ca_v1.3$ II-III loop into $Ca_v1.2$/DHPi not only increased the efficiency of nifedipine-resistant KCl-stimulated insulin secretion (Fig. 6A) but also conferred the ability to mediate nifedipine-resistant, glucose-stimulated insulin secretion (Fig. 7A).

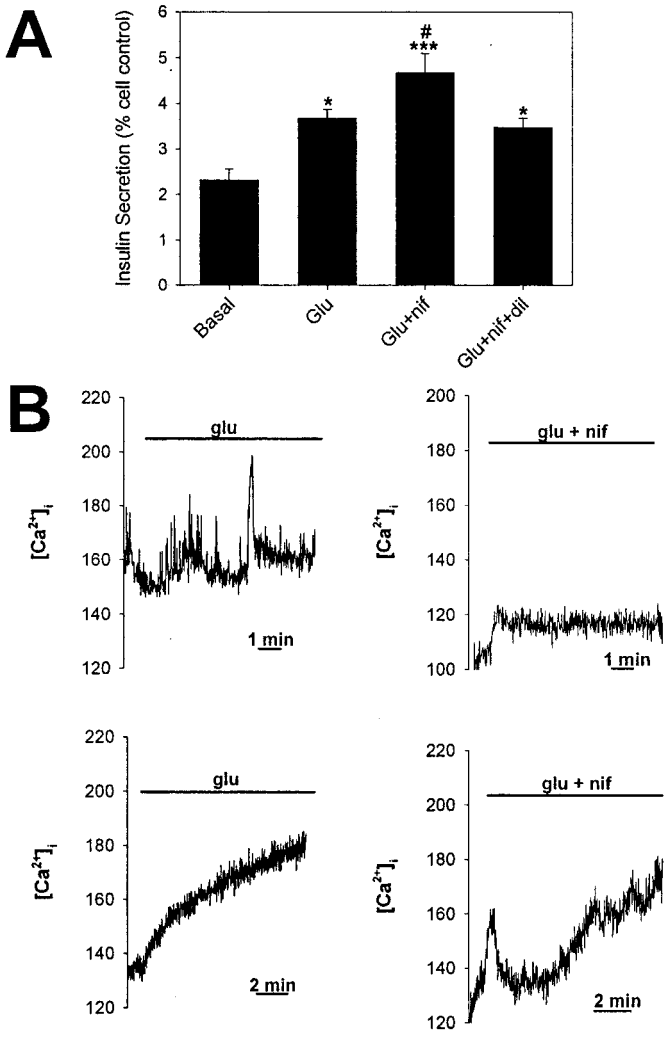

Fig. 7. Insulin secretion and $[Ca^{2+}]_i$ changes in response to glucose in $Ca_v1.2$/DHPi/1.3II-III cells. A, insulin secretion (expressed as the percentage of cell content) in response to 11.2 mM glucose stimulation for $Ca_v1.2$/DHPi/1.3II-III cells: basal = 2.33 ± 0.23%, 11.2 mM glucose (glu) = 3.68 ± 0.19%, 11.2 mM glucose + 10 μM nifedipine (glu + nif) = 4.69 ± 0.42%, and 11.2 mM glucose + 10 μM nifedipine (nif) + 500 μM diltiazem (glu + nif + dil) = 3.48 ± 0.20% (n = 6). Secretion stimulated by 11.2 mM glucose in the absence (glu) and presence of nifedipine (glu + nif) was significantly different from basal secretion (⋆, $p < 0.05$; ⋆⋆⋆, $p < 0.001$, one-way ANOVA with Tukey post hoc test). Secretion in the presence of 11.2 mM glucose + 10 μM nifedipine was significantly different from secretion in the presence of 11.2 mM glucose + 10 μM nifedipine + 500 μM diltiazem (#, $p < 0.05$, one-way ANOVA with Tukey post hoc test). Secretion in the presence of 11.2 mM glucose + 10 μM nifedipine + 500 μM diltiazem (glu + nif + dil) was significantly greater than basal (⋆, $p < 0.05$, one-way ANOVA with Tukey post hoc test). B, $[Ca^{2+}]_i$ increases in response to 18 mM glucose in $Ca_v1.2$/DHPi/1.3II-III cells: representative traces from single cells. Three distinct responses of $[Ca^{2+}]_i$ to 18 mM glucose were observed in $Ca_v1.2$/DHPi/1.3II-III cells in the absence of nifedipine: oscillations (top left, 1 of 17 cells), a slow increase (bottom left, 8 of 17 cells), and no response (data not shown, 8 of 17 cells). In the presence of 10 μM nifedipine, 18 mM glucose elicited either no response (top right, 11 of 18 cells) or a slow increase (bottom right, 7 of 18 cells) in $[Ca^{2+}]_i$. No cells (0 of 18) were observed to undergo $[Ca^{2+}]_i$ oscillations in response to 18 mM glucose in the presence of 10 μM nifedipine.

To further understand the properties of glucose responsiveness in $Ca_v1.2$/DHPi/1.3II-III cells, we examined the glucose-induced $[Ca^{2+}]_i$ changes in these cells. As shown in Fig. 7B, we observed three distinct patterns in these cells. In a substantial fraction of cells (~47%), no response to glucose was observed (data not shown). In a small subset of cells (~6%,) we observed $[Ca^{2+}]_i$ oscillation in response to 18 mM glucose in the absence of nifedipine, similar to those observed in untransfected INS-1, $Ca_v1.2$/DHPi, and $Ca_v1.3$/DHPi cells in the absence of nifedipine (Fig. 7B, top left). However, a third population of cells (~47%) exhibited a slow increase in $[Ca^{2+}]_i$ in response to 18 mM glucose in the absence of nifedipine (Fig. 7B, bottom left). In the presence of 10 μM nifedipine, $[Ca^{2+}]_i$ in the majority of cells (~60%) did not respond to 18 mM glucose (Fig. 7B, top right), whereas ~40% of cells retained the slow increase in $[Ca^{2+}]_i$ (Fig. 7B, bottom right). Thus, insertion of the $Ca_v1.3$ II-III loop into $Ca_v1.2$/DHPi confers the ability to mediate glucose-stimulated increases in $[Ca^{2+}]_i$ that are kinetically distinct from those mediated by the $Ca_v1.3$/DHPi channel (Fig. 2).

Discussion

Glucose-induced $[Ca^{2+}]_i$ oscillations have been observed and intensively studied in pancreatic β cells, but the cellular mechanism and the source of the Ca^{2+} responsible for oscillations are still debated. On the one hand, the oscillatory calcium influx through VDCC driven by oscillations in membrane potential may exclusively account for glucose-induced $[Ca^{2+}]_i$ oscillations. On the other hand, Ca^{2+} release from internal Ca^{2+} stores may directly initiate oscillations or regulate membrane potential (Roe et al., 1993; Gilon et al., 1999; Arredouani et al., 2002). Nonetheless, the $[Ca^{2+}]_i$ oscillation in response to glucose is apparently important for insulin secretion because it is associated with β cell-membrane electrical bursting activity and, according to some studies, pulsatile insulin secretion (Bergsten et al., 1994; Ravier et al., 1999; Kjems et al., 2002). The increase in $[Ca^{2+}]_i$ induced by KCl (Figs. 1B; 2, C and D; and 6B), is consistent with the nonoscillatory release of insulin observed in KCl-stimulated β cells (Kjems et al., 2002). Although KCl causes Ca^{2+} influx by direct membrane depolarization, it is likely that the metabolism of glucose is involved in the glucose-induced $[Ca^{2+}]_i$ oscillation. The observation that nifedipine completely abolished Ca^{2+} transients in response to glucose or KCl stimulation in untransfected INS-1 cells (Fig. 1) indicates the requirement for L-type VDCC activation in both cases.

The capability of both $Ca_v1.2$ and $Ca_v1.3$ channels to mediate KCl-induced $[Ca^{2+}]_i$ elevation (Fig. 2, C and D) and the specificity of $Ca_v1.3$ channels in mediating glucose-induced $[Ca^{2+}]_i$ oscillations (Fig. 2, A and B) are consistent with our previous study of insulin secretion in these cells lines (Liu et al., 2003). The $Ca_v1.3$ II-III loop also increases the efficiency of $Ca_v1.2$/DHPi excitation-secretion coupling in response to KCl (Fig. 6A) in the context of the $Ca_v1.2$/DHPi/1.3II-III chimera. In addition, overexpression of the $Ca_v1.3$ II-III loop uncoupled endogenous L-type channels from both glucose-stimulated insulin secretion (Liu et al., 2003) and glucose-stimulated $[Ca^{2+}]_i$ oscillation (Fig. 4B). Even when the $Ca_v1.3$ II-III loop was introduced in the context of the $Ca_v1.2$/DHPi/1.3II-III chimera, endogenous L-type channels were largely uncoupled from glucose-stimulated $[Ca^{2+}]_i$ oscillation

Downloaded from molpharm.aspetjournals.org at ASPET Journals on February 26, 2020

(Fig. 7B). Finally, the inclusion of the $Ca_v1.3$ II-III loop in the $Ca_v1.2$/DHPi/1.3II-III chimera confers upon $Ca_v1.2$/DHPi the ability to respond to glucose stimulation by mediating both insulin secretion (Fig. 7A) and a slow increase in $[Ca^{2+}]_i$ (Fig. 7B). Taken together, our data suggest that $Ca_v1.3$ is preferentially coupled to glucose-stimulated $[Ca^{2+}]_i$ oscillation in INS-1 cells and that the II-III loop of $Ca_v1.3$ plays a role in this process. We propose that the role of the $Ca_v1.3$ II-III loop is to position the channel in a signaling complex that allows optimal Ca^{2+} influx in response to glucose-induced depolarization and tightly couples Ca^{2+} influx to insulin secretion. The distinct patterns of $[Ca^{2+}]_i$ changes in response to glucose seem to be mediated by molecular determinants distinct from the II-III loop because the II-III loop of $Ca_v1.3$ does not transfer the ability to mediate glucose-induced $[Ca^{2+}]_i$ oscillation to $Ca_v1.2$ (Fig. 7B).

The preferential coupling of $Ca_v1.3$ to glucose-induced $[Ca^{2+}]_i$ oscillation in INS-1 cells may be mediated by any of several possible mechanisms. The voltage-dependence of activation of $Ca_v1.3$ may be more negative than that of $Ca_v1.2$ when expressed in INS-1 cells. However, the $V_{1/2}$ inactivation of the $Ca_v1.2$ and $Ca_v1.3$ clones used in this study are virtually identical when measured in the same expression system (Bell et al., 2001; Gage et al., 2002). Furthermore, we have observed no difference in the voltage-dependence of activation of whole-cell Ba^{2+} currents between untransfected INS-1, $Ca_v1.2$/DHPi, or $Ca_v1.3$/DHPi cells (G. Liu and G. H. Hockerman, unpublished data). Finally, the chimeric $Ca_v1.2$/DHPi/1.3II-III channel is activated by depolarizations induced by glucose stimulation, so unless the insertion of the $Ca_v1.3$ II-III loop significantly shifts the voltage-dependence of activation to more negative potentials, the $Ca_v1.2$/DHPi channel seems capable of opening in response to glucose-induced depolarizations.

Alternatively, $Ca_v1.3$ may be preferentially linked to an intracellular machinery responsible for generating $[Ca^{2+}]_i$ oscillation. The calcium-induced calcium-release channel RYR2 is expressed in β cells and contributes to Ca^{2+} release from ER (Lemmens et al., 2001; Bruton et al., 2003). Therefore, it is possible that a preferential coupling between $Ca_v1.3$ on the plasma membrane and RYR2 on the ER membrane may mediate glucose-induced $[Ca^{2+}]_i$ oscillation. However, thapsigargin, which depletes ER Ca^{2+} stores by inhibiting the ER Ca^{2+} ATPase, does not inhibit either glucose-stimulated insulin secretion (Liu and Hockerman, unpublished results) or $[Ca^{2+}]_i$ oscillations (Herbst et al., 2002) in INS-1 cells. Therefore, at least in the INS-1 cell model, it is not likely that intracellular Ca^{2+} release is required for glucose-stimulated insulin secretion or $[Ca^{2+}]_i$ oscillations. Finally, preferential coupling of $Ca_v1.3$ to glucose-induced Ca^{2+} oscillations could be mediated by coupling of Ca^{2+} influx to other ion conductances on the plasma membrane, leading to fluctuations in membrane potential. For example, experimental observations (Gopel et al., 1999) and models of glucose-stimulated $[Ca^{2+}]_i$ oscillation (Fridlyand et al., 2003) suggest that coupling of Ca^{2+} influx to Ca^{2+}-activated K^+ channels may be part of the mechanism.

Our observation that $Ca_v1.3$ channels can mediate $[Ca^{2+}]_i$ oscillations in INS-1 cells while $Ca_v1.2$ channels cannot contrasts with the essential role of $Ca_v1.2$ in the first phase of insulin secretion in mouse β cells recently demonstrated using a tissue-selective knockout technique (Schulla et al., 2003). However, the predominant L-type VDCC in rat and human β cells is $Ca_v1.3$ (Seino et al., 1992). The differing effectiveness of $Ca_v1.2$ in mediating glucose-stimulated insulin secretion and $[Ca^{2+}]_i$ oscillation in INS-1 cells and mouse β cells is most likely not a result of amino acid differences between mouse and rat $Ca_v1.2$ because mouse $Ca_v1.2$ is virtually identical with the rat brain $Ca_v1.2$ used in this study (Ma et al., 1992). Alternatively, the coupling of different L-type channels to glucose-stimulated events in INS-1 cells (rat) and mouse β cells may reflect a distinct set of signaling proteins downstream of Ca^{2+} entry in these cells capable of coupling to $Ca_v1.3$ and $Ca_v1.2$, respectively. In support of this notion, distinct responses of $[Ca^{2+}]_i$ and membrane potential to glucose stimulation have been reported in mouse and rat islets (Atunes et al., 2000).

Many types of neurons also express both $Ca_v1.2$ and $Ca_v1.3$ channels (Hell et al., 1993a). Whereas distinct functional roles for either channel subtype are not well defined, some studies have suggested parallels between L-type channel function in β cells and neurons. For example, L-type channel activity is modulated in an oscillatory manner by a metabotropic glutamate 1 agonist or caffeine in cerebellar granule cells via a mechanism that is inhibited by ryanodine (Chavis et al., 1996). More recently, L-type channel activation of ryanodine receptors in response to ischemia has been reported in spinal cord white matter (Ouardouz et al., 2003). Interestingly, Ouardouz et al. (2003) found that $Ca_v1.2$ interacts with RYR1, whereas $Ca_v1.3$ interacts with RYR2 as assessed by coimmunoprecipitation. Thus, RYR and L-type channel activity may be functionally coupled in neurons. In addition, Ca^{2+} entry via L-type channels selectively activates small-conductance Ca^{2+}-activated K^+ channels (Marrion and Tavalin, 1998), and $Ca_v1.3$, but not $Ca_v1.2$, channels are reported to colocalize with small-conductance Ca^{2+}-activated K^+ (SK) channels in rat hippocampal neurons (Bowden et al., 2001). On the other hand, activation of $Ca_v1.2$ channels in rat cortical neurons was shown to activate the transcription factor cAMP response element-binding protein and is proposed to modulate gene expression via the mitogen-activated protein kinase pathway (Dolmetsch et al., 2001). Thus, $Ca_v1.2$ and $Ca_v1.3$ channels may be coupled to distinct signaling pathways in neurons as well as in pancreatic β cells.

In summary, we have shown that $Ca_v1.3$ is preferentially linked to glucose-triggered $[Ca^{2+}]_i$ oscillation in INS-1 cells, which is proposed as the potential mechanism for the observed coupling of $Ca_v1.3$ to glucose-induced insulin exocytosis in these cells. It will be of interest to determine whether the inclusion of other divergent domains besides or in addition to the II-III loop of $Ca_v1.3$ can confer upon $Ca_v1.2$ the ability to mediate glucose-stimulated $[Ca^{2+}]_i$ oscillation in INS-1 cells. Our results extend the potential application of drug-insensitive channels in the study of channel-mediated cellular events and suggest their use for the delineation of specific roles for $Ca_v1.2$ and $Ca_v1.3$ in other cell types in which both channels are expressed.

Acknowledgments

The human brain $Ca_v1.3$ clone was provided by SIBIA Neurosciences Inc. (San Diego, CA), which is now Merck Research Labs (West Point, PA). The antibody directed against the C-terminal tail of $Ca_v1.2$ (CNC2) was a gift from Dr. William A. Catterall. Ca^{2+}

Downloaded from molpharm.aspetjournals.org at ASPET Journals on February 26, 2020

imaging experiments were carried out at the Purdue University Cytometry Laboratories.

References

Arredouani A, Guiot Y, Jonas JC, Liu LH, Nenquin M, Pertusa JA, Rahier J, Rolland JF, Shull GE, Stevens M, et al. (2002) SERCA3 ablation does not impair insulin secretion but suggests distinct roles of different sarcoendoplasmic reticulum Ca^{2+} pumps for Ca^{2+} homeostasis in pancreatic beta-cells. *Diabetes* **51:**3245–3253.

Asfari M, Janjic D, Meda P, Li G, Halban PA, and Wollheim CB (1992) Establishment of 2-mercaptoethanol-dependent differentiated insulin-secreting cell lines. *Endocrinology* **130:**167–178.

Atunes CM, Salgado AP, and Rosario RM (2000) Differential patterns of glucose-induced electrical activity and intracellular calcium response in single mouse and rat pancreatic islets. *Diabetes* **49:**2028–2038.

Bell DC, Butcher AJ, Berrow NS, Page KM, Brust PF, Nesterova A, Stauderman KA, Seabrook GR, Nurnberg B, and Dolphin AC (2001) Biophysical properties, pharmacology and modulation of human, neuronal L-type ($alpha_{1D}$, $Ca_V1.3$) voltage-dependent calcium currents. *J Neurophysiol* **85:**816–827.

Bergsten P (1998) Glucose-induced pulsatile insulin release from single islets at stable and oscillatory cytoplasmic Ca^{2+}. *Am J Physiol* 274:E796–E800.

Bergsten P, Grapengiesser E, Gylfe E, Tengholm A, and Hellman B (1994) Synchronous oscillations of cytoplasmic Ca^{2+} and insulin release in glucose-stimulated pancreatic islets. *J Biol Chem* **269:**8749–8753.

Bowden SE, Fletcher S, Loane DJ, and Marrion NV (2001) Somatic colocalization of rat SK1 and D class ($Ca_v1.3$) L-type calcium channels in rat CA1 hippocampal pyramidal neurons. *J Neurosci* **21:**RC175–RC175.

Bruton JD, Lemmens R, Shi CL, Persson-Sjogren S, Westerblad H, Ahmed M, Pyne NJ, Frame M, Furman BL, and Islam MS (2003) Ryanodine receptors of pancreatic beta-cells mediate a distinct context-dependent signal for insulin secretion. *FASEB J* **17:**301–303.

Chavis P, Fagni L, Lansman JB, and Bockaert J (1996) Functional coupling between ryanodine receptors and L-type calcium channels in neurons. *Nature (Lond)* **382:** 719–722.

Devis G, Somers G, and Malaisse WJ (1975a) Stimulation of insulin release by calcium. *Biochem Biophys Res Commun* **67:**525–529.

Devis G, Somers G, Van Obberghen E, and Malaisse WJ (1975b) Calcium antagonists and islet function. I. Inhibition of insulin release by verapamil. *Diabetes* **24:**247–251.

Dolmetsch RE, Pajvani U, Fife K, Spotts JM, and Greenberg ME (2001) Signaling to the nucleus by an L-type Ca^{2+} channel-calmodulin complex through the MAP kinase pathway. *Science (Wash DC)* **294:**333–339.

Dukes ID and Cleemann L (1993) Calcium current regulation of depolarization-evoked calcium transients in beta-cells (HIT-T15). *Am J Physiol* **264:**E348–E353.

Fridlyand LE, Tamarina N, and Philipson LH (2003) Modeling of Ca^{2+} flux in pancreatic {beta}-cells: role of the plasma membrane and intracellular stores. *Am J Physiol* **285:**E138–E154.

Gage MJ, Rane SG, Hockerman GH, and Smith TJ (2002) The virally encoded fungal toxin KP4 specifically blocks L-type voltage-gated calcium channels. *Mol Pharmacol* **61:**936–944.

Gilon P, Arredouani A, Gailly P, Gromada J, and Henquin JC (1999) Uptake and release of Ca^{2+} by the endoplasmic reticulum contribute to the oscillations of the cytosolic Ca^{2+} concentration triggered by Ca^{2+} influx in the electrically excitable pancreatic B-cell. *J Biol Chem* **274:**20197–20205.

Gopel SO, Kanno T, Barg S, Eliasson L, Galvanovskis J, Renstrom E, and Rorsman P (1999) Activation of Ca^{2+}-dependent K^+ channels contributes to rhythmic firing of action potentials in mouse pancreatic beta cells. *J Gen Physiol* **114:**759–770.

Grapengiesser E, Gylfe E, and Hellman B (1992) Glucose sensing of individual pancreatic beta-cells involves transitions between steady-state and oscillatory cytoplasmic Ca^{2+}. *Cell Calcium* **13:**219–226.

Hell JW, Westenbroek RE, Warner C, Ahlijanian MK, Prystay W, Gilbert MM, Snutch TP, and Catterall WA (1993a) Identification and differential subcellular localization of the neuronal class c and class d l-type calcium channel alpha 1 subunits. *J Cell Biol* **123:**949–962.

Hell JW, Yokoyama CT, Wong ST, Warner C, Snutch TP, and Catterall WA (1993b) Differential phosphorylation of two size forms of the neuronal class c l-type calcium channel alpha 1 subunit. *J Biol Chem* **268:**19451–19457.

Hellman B, Gylfe E, Bergsten P, Grapengiesser E, Lund PE, Berts A, Tengholm A, Pipeleers DG, and Ling Z (1994) Glucose induces oscillatory Ca^{2+} signalling and insulin release in human pancreatic beta cells. *Diabetologia* **37 Suppl 2:**S11–S20.

Herbst M, Sasse P, Greger R, Yu H, Heschler J, and Ullrich S (2002) Membrane potential dependent modulation of calcium oscillations in insulin secreting INS-1 cells. *Cell Calcium* **31:**115–126.

Horvath A, Szabadkai G, Varnai P, Aranyi T, Wollheim CB, Spat A, and Enyedi P (1998) Voltage dependent calcium channels in adrenal glomerulosa cells and in insulin producing cells. *Cell Calcium* **23:**33–42.

Islam MS, Rorsman P, and Berggren PO (1992) Ca^{2+}-induced Ca^{2+} release in insulin-secreting cells. *FEBS Lett* **296:**287–291.

Kjems LL, Ravier MA, Jonas JC, and Henquin JC (2002) Do oscillations of insulin secretion occur in the absence of cytoplasmic Ca^{2+} oscillations in beta-cells? *Diabetes* **51 Suppl 1:**S177–S182.

Larsson O, Kindmark H, Brandstrom R, Fredholm B, and Berggren PO (1996) Oscillations in K_{ATP} channel activity promote oscillations in cytoplasmic free Ca^{2+} concentration in the pancreatic beta cell. *Proc Natl Acad Sci USA* **93:**5161–5165.

Lemmens R, Larsson O, Berggren PO, and Islam MS (2001) Ca^{2+}-induced Ca^{2+} release from the endoplasmic reticulum amplifies the Ca^{2+} signal mediated by activation of voltage-gated L-type Ca^{2+} channels in pancreatic beta-cells. *J Biol Chem* **276:**9971–9977.

Liu G, Dilmac N, Hilliard N, and Hockerman GH (2003) $Ca_v1.3$ is preferentially coupled to glucose-stimulated insulin secretion in the pancreatic beta-cell line INS-1. *J Pharmacol Exp Ther* **305:**271–278.

Ma W-J, Holz RW, and Uhler MD (1992) Expression of a cDNA for a neuronal calcium channel $\alpha 1$ subunit enhances secretion from adrenal chromaffin cells. *J Biol Chem* **267:**22728–22732.

Marrion NV and Tavalin SJ (1998) Selective activation of Ca^{2+}-activated K^+ channels by co-localized Ca2+ channels in hippocampal neurons. *Nature (Lond)* **395:** 900–905.

Ouardouz M, Nikolaeva MA, Coderre E, Zamponi GW, McRory JE, Trapp BD, Yin X, Wang W, Woulfe J, and Stys PK (2003) Depolarization-induced Ca^{2+} release in ischemic spinal cord white matter involves L-type Ca^{2+} channel activation of ryanodine receptors. *Neuron* **40:**53–63.

Peterson BZ, Johnson BD, Hockerman GH, Acheson M, Scheuer T, and Catterall WA (1997) Analysis of the dihydropyridine receptor site on L-type Ca^{2+} channels by alanine scanning mutagenesis. *J Biol Chem* **272:**18752–18758.

Ravier MA, Gilon P, and Henquin JC (1999) Oscillations of insulin secretion can be triggered by imposed oscillations of cytoplasmic Ca^{2+} or metabolism in normal mouse islets. *Diabetes* **48:**2374–2382.

Roe MW, Lancaster ME, Mertz RJ, Worley JF 3rd, and Dukes ID (1993) Voltage-dependent intracellular Ca^{2+} release from mouse islets stimulated by glucose. *J Biol Chem* **268:**9953–9956.

Roe MW, Worley JF 3rd, Qian F, Tamarina N, Mittal AA, Dralyuk F, Blair NT, Mertz RJ, Philipson LH, and Dukes ID (1998) Characterization of a Ca^{2+} release-activated nonselective cation current regulating membrane potential and $[Ca^{2+}]_i$ oscillations in transgenically derived beta-cells. *J Biol Chem* **273:**10402–10410.

Schulla V, Renström E, Feil R, Feil S, Franklin I, Gjinovci A, Jing X-J, Laux D, Lundquist I, Magnuson MA, et al. (2003) Impaired insulin secretion and glucose tolerance in β cell-selective $Ca_v1.2$ Ca^{2+} channel null mice. *EMBO (Eur Mol Biol Organ) J* **22:**3844–3854.

Seino S, Chen L, Seino M, Blondel O, Takeda J, Johnson JH, and Bell GI (1992) Cloning of the alpha 1 subunit of a voltage-dependent calcium channel expressed in pancreatic beta cells. *Proc Natl Acad Sci USA* **89:**584–588.

Soria B and Martin F (1998) Cytosolic Ca^{2+} oscillations and insulin release in pancreatic islets of Langerhans. *Diabetes Metab* **24:**37–40.

Theler JM, Mollard P, Guerineau N, Vacher P, Pralong WF, Schlegel W, and Wollheim CB (1992) Video imaging of cytosolic Ca^{2+} in pancreatic beta-cells stimulated by glucose, carbachol and ATP. *J Biol Chem* **267:**18110–18117.

Westerlund J, Gylfe E, and Bergsten P (1997) Pulsatile insulin release from pancreatic islets with nonoscillatory elevation of cytoplasmic Ca^{2+}. *J Clin Investig* **100:** 2547–2551.

Address correspondence to: Dr. Gregory Hockerman, 575 Stadium Mall Drive, West Lafayette, IN 47907-2091. E-mail: gregh@pharmacy.purdue.edu

Downloaded from molpharm.aspetjournals.org at ASPET Journals on February 26, 2020